

organic end groups and perhaps many inorganic end groups will stabilize linear carbon.

REFERENCES AND NOTES

1. E. Edelson, *Mosaic* **23**, 2 (1992); R. Hoffmann, *Tetrahedron* **22**, 521 (1966); _____, T. Hughbanks, M. Kertesz, *J. Am. Chem. Soc.* **105**, 4831 (1983).
2. A form of carbon called "carbyne" has been reported (3), but other workers have extensively studied their evidence (4–7) and this contention is generally held to be incorrect.
3. V. M. Mel'nichenko, B. N. Smirnov, V. P. Varlakov, Y. N. Nikulin, A. M. Sladkov, *Carbon* **21**, 131 (1983), and references contained therein.
4. P. P. K. Smith and P. R. Buseck, *Science* **216**, 984 (1982).
5. J. Jansta, F. P. Dousek, V. Patazelova, *Carbon* **13**, 377 (1975).
6. W. A. Little, *Phys. Rev.* **134**, 1416 (1964).
7. M. F. Hawthorne, *Preliminary Reports, Memoranda and Technical Notes of the Materials Research Council Summer Conference* (National Technical Information Service, Springfield, VA, 1973).
8. R. Eastmond, T. R. Johnston, D. R. M. Walton, *Tetrahedron* **28**, 4601 (1972).
9. A more detailed study is planned. It appears that such radical-terminated species are unstable above -100°C .
10. F. Diederich *et al.*, *Science* **245**, 1088 (1989).
11. F. Diederich *et al.*, *J. Am. Chem. Soc.* **113**, 6943 (1991).
12. H. G. Viehe, *Chem. Ber.* **92**, 1270 (1959).
13. E. A. Rohlfing, D. M. Cox, A. Kaldor, *J. Chem. Phys.* **81**, 3322 (1984).
14. R. E. Smalley *et al.*, *J. Am. Chem. Soc.* **109**, 359 (1987).
15. T. Grösser and A. Hirsch, *Angew. Chem. Int. Ed. Engl.* **32**, 1340 (1993).
16. W. Krätschmer, L. D. Lamb, K. Fostiropoulos, D. R. Huffman, *Nature* **347**, 354 (1990).
17. J. A. Morrison and R. J. Lagow, *Adv. Inorg. Radiochem.* **23**, 177 (1979); T. R. Bierschenk, M. A. Guerra, T. J. Juhlke, S. B. Larson, R. J. Lagow, *J. Am. Chem. Soc.* **109**, 4855 (1987).
18. A. Kaldor, D. M. Cox, K. C. Reichmann, *J. Chem. Phys.* **88**, 1588 (1988).
19. G. von Helden, M. T. Hsu, P. R. Kemper, M. T. Bowers, *ibid.* **95**, 3835 (1991).
20. J. Hunter, J. Fye, M. F. Jarrold, *Science* **260**, 784 (1993); J. M. Hunter, J. L. Fye, E. J. Roskamp, M. F. Jarrold, *J. Phys. Chem.* **98**, 1810 (1994).
21. C. A. Wilkie and D. T. Haworth, *J. Inorg. Nucl. Chem.* **40**, 1989 (1978).
22. The R.J.L. laboratory is grateful for substantial support from the U.S. Department of Energy Advanced Research Projects Agency grant DE-FG05-91ER12119, the Air Force Office of Scientific Research grant F49620-92-J-0104, the National Science Foundation grant CHE-9106482, and the Robert A. Welch Foundation grant F-0700.

19 July 1994; accepted 17 October 1994

Visualization of Surfactants on Nanostructured Palladium Clusters by a Combination of STM and High-Resolution TEM

Manfred T. Reetz,* Wolfgang Helbig, Stefan A. Quaiser, Ulrich Stimming, Norbert Breuer, Roland Vogel

Scanning tunneling microscopy (STM) and high-resolution transmission electron microscopy (TEM) have been used to determine the dimensions of a series of palladium clusters stabilized by tetraalkylammonium salts. Electrochemically prepared colloids were used in which the average diameter of the inner metal core was varied between 2 and 4 nanometers, and the size of the ammonium ions was adjusted in the series ${}^+\text{N}(\text{n}-\text{C}_4\text{H}_9)_4 < {}^+\text{N}(\text{n}-\text{C}_8\text{H}_{17})_4 < {}^+\text{N}(\text{n}-\text{C}_{18}\text{H}_{37})_4$. The difference between the mean diameter determined by STM and that measured by TEM allows the determination of the thickness of the protective surfactant layer. On the basis of these studies, a model of the geometric properties of ammonium-stabilized palladium clusters has been proposed. Suggestions for the mechanism of the STM imaging process are also made.

Current interest in metal clusters and colloids in the size range of 1 to 10 nm is increasing because of their actual and potential use as catalysts and as advanced materials in electronics (1). In order to prevent agglomeration with the formation of large particles or powders, these nanostructured clusters usually need to be protected by stabilizers such as polymers

(for example, polyvinylpyrrolidone) (2), ligands (for example, phenanthroline) (3), or surfactants (for example, tetraalkylammonium salts) (4). Synthetic routes include metal vaporization and chemical reduction of metals salts in the presence of the stabilizers (1–4). In most cases, the nature of stabilization is not well understood (5), and knowledge of the actual structure and dimensions of the materials is limited. Generally, high-resolution transmission electron microscopy (TEM) has been used, but this technique provides only information regarding the size of the metal cores (6). Because scanning tunneling microscopy (STM) is a powerful tool for the character-

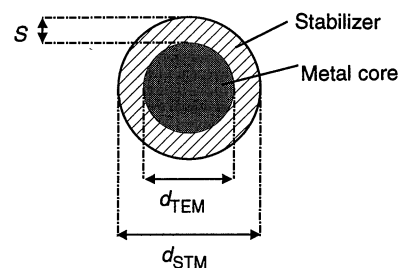


Fig. 1. Schematic diagram defining the terms used in this study.

ization of surfaces and catalysts (7), it might be expected to be useful in the determination of the outer dimensions of the actual colloidal materials. The difference between the mean diameter determined by each of these methods, d_{STM} and d_{TEM} , would be $2S$, where S is the thickness of the protective layer (Fig. 1). Previous STM studies of gold and Pd clusters stabilized by phenanthroline derivatives have culminated in the gross characterization of the surface topography, but so far, details regarding d_{STM} have not been possible (8).

We have recently described the size-selective electrochemical synthesis of tetraalkylammonium-stabilized Pd and Ni clusters: Control of particle size (d_{TEM}) is possible by simple adjustment of the current density (9). Because the bulkiness of tetraalkylammonium ions ${}^+\text{NR}_4$ can be varied by the proper choice of R groups, we have a simple experimental method for the systematic preparation of ammonium-stabilized clusters in which the geometric parameters (Fig. 1) can be varied at will. In this report, we present the results of a study combining STM and high-resolution TEM of stabilized metal clusters. Direct measurements of d_{STM} and d_{TEM} for a series of tetraalkylammonium-stabilized Pd clusters is provided, allowing a fairly detailed study of the interaction between tetraalkylammonium ions and metal clusters.

A series of Pd clusters was synthesized as previously described (9). We prepared the samples for the TEM studies by dip coating a commercially available TEM grid (400 mesh, copper with 5-nm amorphous carbon) with $\sim 10^{-4}$ M solutions of the colloids. The images were taken at a magnification of 3×10^5 with a Hitachi HF2000 high-resolution TEM at an acceleration voltage of 200 keV. Materials with different d_{TEM} values but with the ammonium salt remaining the same were investigated, along with materials in which the d_{TEM} values were approximately constant but the size of ammonium ions varied (Table 1). The clusters were then studied by STM. Substrates for the STM measurements were quartz slides with vapor-deposited gold films 200 nm thick. An essential step necessary

M. T. Reetz, W. Helbig, S. A. Quaiser, Max-Planck-Institut für Kohlenforschung, Kaiser-Wilhelm-Platz 1, D-45470 Mülheim/Ruhr, Germany.

U. Stimming, N. Breuer, R. Vogel, Forschungszentrum Jülich, Institut für Energieverfahrenstechnik, D-52424 Jülich, Germany.

*To whom correspondence should be addressed.

for successful imaging is a flame annealing process, which leads to a smooth gold surface with atomic steps and large, atomically flat terraces. The colloids were then attached to the surface by dip coating with the colloidal solution. The STM measure-

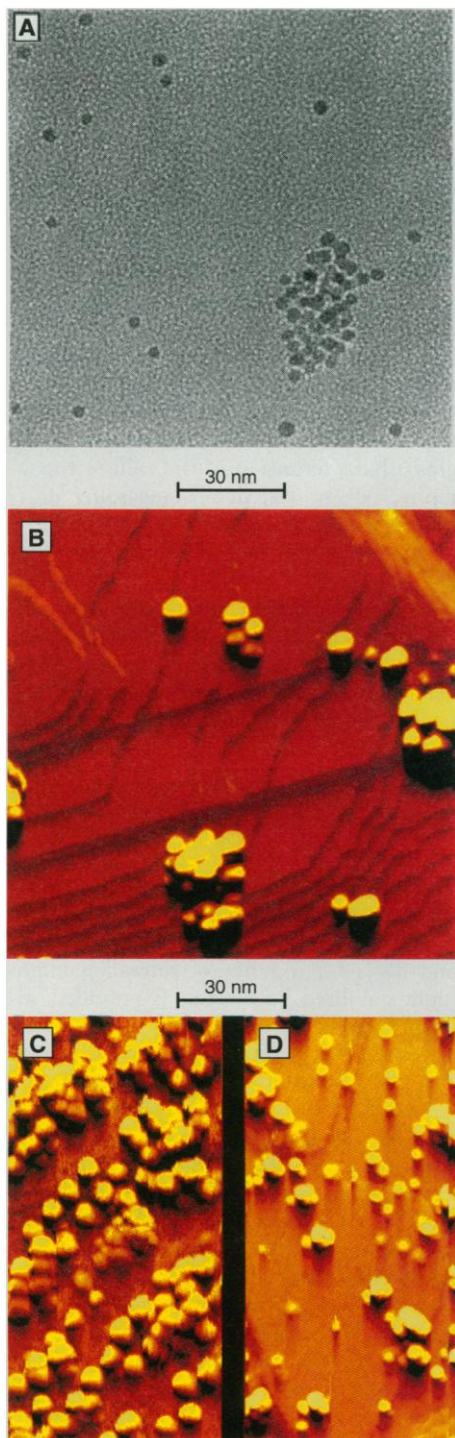


Fig. 2. (A) A high-resolution TEM of a 4.1-nm Pd colloid stabilized by $N(n\text{-C}_8\text{H}_{17})_4\text{Br}$. (B) STM image of the same colloid. (C) STM image of another $N(n\text{-C}_8\text{H}_{17})_4\text{Br}$ -stabilized colloid ($d_{\text{STM}} = 6.9$ nm; $d_{\text{TEM}} = 4.1$ nm). (D) STM image of a third $N(n\text{-C}_8\text{H}_{17})_4\text{Br}$ -stabilized colloid ($d_{\text{STM}} = 4.0$ nm; $d_{\text{TEM}} = 2.0$ nm).

ments were performed with a "beetle" type STM (10). Etched Pt-Ir wires (90% Pt, 10% Ir) were used as tips.

A typical high-resolution TEM image of a Pd cluster stabilized by $N(n\text{-C}_4\text{H}_9)_4\text{Br}$ (Fig. 2A) yields an average diameter d_{TEM} of 4.1 nm. The STM image (Fig. 2B) reveals particles with an average diameter d_{STM} of 6.9 nm. Similar studies were performed with

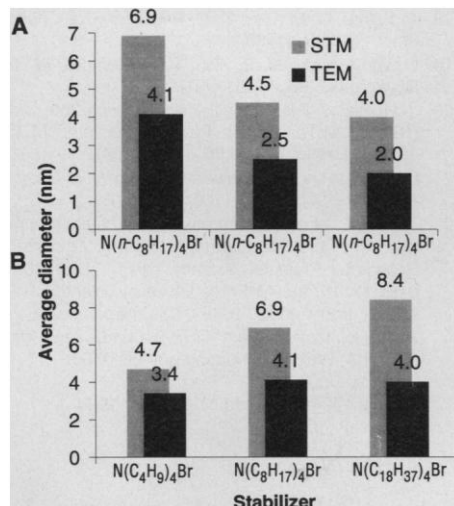


Fig. 3. (A) Influence of the metal core size on the STM image [stabilizer: $N(n\text{-C}_8\text{H}_{17})_4\text{Br}$]. (B) Influence of the stabilizer size on the STM image.

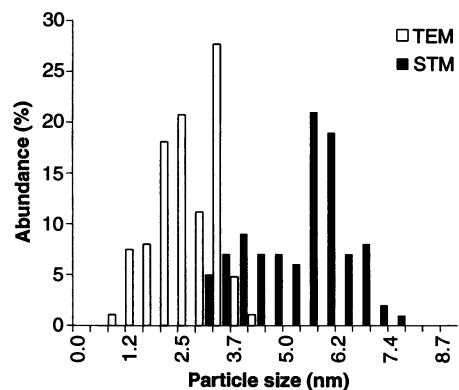


Fig. 4. Size distribution diagrams of a 2.5-nm $N(n\text{-C}_8\text{H}_{17})_4\text{Br}$ -stabilized cluster.

Table 1. Electrochemically prepared Pd colloids. The first three rows refer to materials with different values of d_{TEM} but with the same ammonium salt. For the last three rows, d_{TEM} is approximately constant, but the size of the ammonium ions vary. In all cases, the electrolyte used was a 0.1 M solution in acetonitrile (ACN) or tetrahydrofuran (THF). The current and temperature varied as noted. The last column gives a solvent in which the colloid is soluble: THF, N,N -dimethylformamide (DMF), or pentane.

d_{TEM} (nm)	Electrolyte	Conditions		Colloid soluble in
		Current (mA/cm ²)	Temperature (°C)	
2.0	$N(n\text{-C}_8\text{H}_{17})_4\text{Br}$ in ACN	4	20	THF
2.5	$N(n\text{-C}_8\text{H}_{17})_4\text{Br}$ in ACN	1	20	THF
4.1	$N(n\text{-C}_8\text{H}_{17})_4\text{Br}$ in ACN	0.2	20	THF
3.4	$N(n\text{-C}_4\text{H}_9)_4\text{Br}$ in THF	4	30	DMF
4.0	$N(n\text{-C}_{18}\text{H}_{37})_4\text{Br}$ in THF	4	50	Pentane

the other materials. Typical STM images are shown in Fig. 2, C and D. In each image, about 100 particles were used for the determination of the average particle diameters. In all cases, d_{STM} turned out to be larger than d_{TEM} (Fig. 3).

The geometric difference ($d_{\text{STM}} - d_{\text{TEM}}$) in the series of $N(n\text{-C}_8\text{H}_{17})_4\text{Br}$ -stabilized clusters is nearly independent of the metal core diameter d_{TEM} (Fig. 3A); that is, STM shows particles that are 2.0 to 2.7 nm larger than the same ones imaged by high-resolution TEM. Thus, one and the same surfactant contributes to the constant difference. Because of the influence of stabilizer size on the STM image (Fig. 3B), $d_{\text{STM}} - d_{\text{TEM}}$ is directly dependent on the size of the ammonium ion, that is, on the length of the alkyl groups in $^+\text{NR}_4$. The STM and TEM size distribution diagrams for the $N(n\text{-C}_8\text{H}_{17})_4\text{Br}$ -stabilized colloid having d_{TEM} of 2.5 nm (Fig.

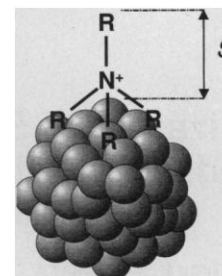


Fig. 5. Model for the interaction of tetraalkylammonium ions with Pd clusters.

Table 2. Calculated and experimental values of stabilizer thickness S for different R groups. The observed values are averages over 100 particles.

R	S (nm)	
	Calculated	Observed
C_4H_9	0.70	0.65
C_8H_{17}	1.10	1.20*
$\text{C}_{18}\text{H}_{37}$	2.40	2.20

*Average value of all measured samples in the $N(n\text{-C}_8\text{H}_{17})_4\text{Br}$ series.

4) complement one another, except that STM makes very small particles (<1 nm) visible, which is not possible by TEM.

Wiesner *et al.* have postulated stabilizing electrostatic interaction between cetyltrimethylammonium ions and Ag surfaces (5). Assuming this general model and placing the H atoms of the α -methylene groups of the $^+NR_4$ ions at the outer surface of the metal core (Fig. 5), it is possible to calculate approximate values of S with standard MM2 force field calculations. The agreement between calculated and experimental values is excellent (Table 2). Thus, a monomolecular protective coat is involved. The results demonstrate that STM is a suitable tool for the visualization of surfactant layers on metal colloids and that the combination STM and high-resolution TEM leads to valuable information regarding the approximate geometric relation between the metal core and the stabilizing mantle. It is likely that the method of combined STM-TEM is not restricted to our materials.

The question remains how the results can be explained in terms of the STM imaging process. The STM images clearly show that the tip is withdrawn from the surface when it reaches a surfactant-covered metal cluster. The feedback mechanism of the STM holds the conductance between tip and sample at a constant value. Thus, the motion of the tip is along a line of constant tunnel resistance. Because the particles are imaged correctly regarding their size, the transfer of electrons through the surfactant layer must be fast and not dependent on the length of the carbon chain of the surfactant. The physical reason for this surprising result is not yet clear and has to be investigated further.

REFERENCES AND NOTES

- G. Schmid, *Clusters and Colloids* (VCH, Weinheim, Germany, 1994); H. Weller, *Angew. Chem.* **105**, 43 (1993) [*Angew. Chem. Int. Ed. Engl.* **32**, 41 (1993)]; S. C. Davis and K. J. Klabunde, *Chem. Rev.* **82**, 153 (1982); L. N. Lewis, *ibid.* **93**, 2693 (1993); B. C. Gates, L. Gucci, H. Knözinger, *Metal Clusters in Catalysis* (Elsevier, Amsterdam, 1986).
- J. S. Bradley, J. M. Millar, E. W. Hill, *J. Am. Chem. Soc.* **113**, 4016 (1991).
- G. Schmid, B. Morun, J.-O. Malm, *Angew. Chem. Lett.* **101**, 772 (1989) [*Angew. Chem. Int. Ed. Engl.* **28**, 778 (1989)]; M. N. Vargaftik, V. P. Zagorodnikov, I. P. Stolarov, I. I. Moiseev, *J. Mol. Catal.* **53**, 315 (1989).
- J. Kiwi and M. Grätzel, *J. Am. Chem. Soc.* **101**, 7214 (1979); Y. Sasson, A. Zoran, J. Blum, *J. Mol. Catal.* **11**, 293 (1981); M. Boutonnet, J. Kizling, R. Touroude, G. Maire, P. Stenius, *Appl. Catal.* **20**, 163 (1986); N. Tushima, T. Takahashi, G. Hirai, *Chem. Lett.* **1985**, 1245 (1985); K. Meguro, M. Torizuka, K. Esumi, *Bull. Chem. Soc. Jpn.* **61**, 341 (1988); N. Satoh and K. Kimura, *ibid.* **62**, 1758 (1989); H. Bönemann *et al.*, *Angew. Chem.* **103**, 1344 (1991) [*Angew. Chem. Int. Ed. Engl.* **30**, 1312 (1991)]; N. Tushima and T. Takahashi, *Bull. Chem. Soc. Jpn.* **65**, 400 (1992).
- J. Wiesner, A. Wokaun, H. Hoffmann, *Prog. Colloid Polym. Sci.* **76**, 271 (1988).
- G. Schmid and co-workers have studied a $P(p-C_6H_4SO_3Na)_2$ -protected gold colloid on a graphite surface by TEM [G. Schmid, *Chem. Rev.* **92**, 1709 (1992)].
- G. Binnig, H. Rohrer, C. Gerber, E. Weibel, *Appl. Phys. Lett.* **40**, 178 (1982); J. Frommer, *Angew. Chem.* **104**, 1325 (1992) [*Angew. Chem. Int. Ed. Engl.* **31**, 1298 (1992)].
- H. A. Wierenga *et al.*, *Adv. Mater.* **2**, 482 (1990); L. E. C. van de Leemput *et al.*, *J. Vac. Sci. Technol. B* **9**, 814 (1991).
- M. T. Reetz and W. Helbig, *J. Am. Chem. Soc.* **116**, 7401 (1994).
- K. Besocke, *Surf. Sci.* **181**, 145 (1987).

14 July 1994; accepted 6 October 1994

The Structure of Confined Oxygen in Silica Xerogels

B. S. Schirato,* M. P. Fang, P. E. Sokol,† S. Komarneni

The microscopic structure of oxygen confined in silica xerogels has been studied as a function of temperature. In large pores, a crystalline solid forms with a structure consistent with that of the bulk. The size of the crystallites is much larger than the pore size, indicating that cooperative effects among pores are important in freezing. As the pore size is decreased, a crossover occurs where solidification results in an amorphous phase in the pores. The resulting amorphous phase is solid but is less ordered than the liquid phase.

The confinement of liquids in restricted geometries leads to many new and interesting features (1). The interactions between molecules and surfaces in interconnected, random confining pores lead to many effects that are of fundamental interest. These effects are also of practical importance in areas such as interfacial adhesion, lubrication, rheology, and tribology.

Previous studies of freezing in porous media have shown significant deviations from bulk freezing (2–5), such as a depression of the freezing temperature and a large hysteresis between cooling and warming. The dynamical properties of the supercooled liquid are also different from those of conventional bulk liquids (2, 6). Recent computer simulations of freezing in confined geometries (7, 8) have resulted in enhanced, rather than suppressed, freezing temperatures. These simulations have also revealed structures different from the bulk that have been observed experimentally in some systems (8).

In this report, we present measurements of the static structure factor $S(Q)$ of oxygen confined in silica xerogels. The microscopic structure of the liquid or solid in the pores, which is reflected in $S(Q)$, is fundamental to obtaining an understanding of the effects of confinement, randomness, and geometrical interconnection on the properties of condensed phases in the pores. Xerogels (9) are porous materials with pore sizes ranging from 10 to 500 Å formed by the gelation

and compaction of silica solutions. They provide a convenient and well-characterized confining medium, and oxygen provides an interesting system for structural studies because it possesses both liquid-solid and solid-solid phase transitions (10), its structure is well known (11–13), and several previous studies of the behavior of oxygen adsorbed in xerogels exist (2, 8, 14). In addition, oxygen is weakly interacting, with respect to the xerogel glass, so that structural changes in the confining material do not occur.

We find that a crystalline solid forms in large pores with a structure consistent with that of the bulk system. The crystallite size of the solid in the pores is much larger than the pore size, indicating that freezing is a cooperative process involving interconnected pores. In small pores, unusual behavior is observed at the liquid-solid transition where solidification results in an amorphous solid phase that is less ordered than the liquid phase.

The xerogels were synthesized in a closed system by mixing 10 ml of tetramethylorthosilicate (TMOS) with 6 ml of various concentrations of HF and NaF with a H_2O /TMOS ratio of 4.96. No alcohol was added. Xerogels with pore diameters of 35, 45, and 60 Å were prepared with 0.1 M HF, 0.2 M HF, and 0.1 M NaF, respectively. The mixed solutions were stirred in airtight containers until gelation occurred. After gelation, gels were left in their respective bottles for about 12 hours before drying at 60° to 65°C for 2 days, which was followed by further drying at 200°C for 4 hours to obtain xerogels. The three gels were then characterized by water and nitrogen adsorption isotherms.

The neutron diffraction measurements were carried out with the Electron Volt

B. S. Schirato, M. P. Fang, P. E. Sokol, Department of Physics, Pennsylvania State University, University Park, PA 16802, USA.

S. Komarneni, Materials Research Laboratory, Pennsylvania State University, University Park, PA 16802, USA.

*Present address: Department of Physics, Cornell University, Clark Hall, Ithaca, NY 14853, USA.

†To whom correspondence should be addressed.